Corrosion Behavior and Failure Mechanism of Rock Bolt(Cable) in Underground Coal Mine

Qiong Wang (wq1989@126.com)
China University of Mining and Technology https://orcid.org/0000-0002-5032-552X

Aiwu Ren
Institut vidnovluvanoi energetiki Nacional'na akademia nauk Ukraini

Songyang Yin
China University of Mining and Technology School of Mechanics and Civil Engineering

Mengyi Li
China University of Mining and Technology

Research

Keywords: Prestressed rock bolt, stress corrosion cracking, corrosion behavior, underground coal mine

Posted Date: July 30th, 2020

DOI: https://doi.org/10.21203/rs.3.rs-47450/v1

Corrosion behavior and failure mechanism of rock bolt(cable) in underground coal mine

Qiong Wang[1,*], Aiwu Ren[2], ,Songyang Yin[3] , Mengyi Li[3]

1 *Department of Emergency Technology and Management，North China Institute of Science & Technology，Beijing 101601，China；*

2 *China Renewable Energy Engineering Institute, Beijing 100120, China；*

3 *School of Mechanics and Civil Engineering, China University of Mining & Technology, Beijing 100083, China.*

Abstract Premature failure of rock bolt (cable) due to stress corrosion cracking (SCC) is a phenomenon that has reported to occur in underground environments. In this study, the corrosion behavior and failure mechanism of rock bolt (cable) samples obtained from underground coal mine were examined and discussed. Macroscopic observation and weight loss test were carried out for the corrosion characteristics of the bolts without failure. It is found the corrosion form is uniform corrosion for the bolts with short service time (S-1, S-2). But for the bolts with longer service time (S-3, S-4 and S-5), experience different degrees of pitting corrosion and the number of corrosion spots on the surface of the sample increases with increase of the service time. The corrosion amount of different parts of the bolts shows the rule of bolt head > bolt end > free section, and the corrosion amount increases year by year with the service time, but the corrosion growth rate is fast in the early stage and slows down in the later stage. At the same time, the failure mechanism of the failure sample S-6, which has been in service for 6 years, was analyzed with macro and micro methods. The results show that S-6 have been in O, Cl and S surrounding rock environment for a long time, resulting serious pitting corrosion and spalling of the surface material of the steel strand, which reduces the outer diameter of the rock cable and its bearing capacity, finally leads to the instantaneous SCC fracture of the sample S-6.

Keywords: Prestressed rock bolt; stress corrosion cracking; corrosion behavior; underground coal mine

1 Introduction

The prestressed rock bolt (cable) technology has been used for more than 80 years since 1934 (Hu et al.1987), and is widely applied in geotechnical engineering for its advantages like light structure, flexible layout, fast construction and low cost (Zhang et al. 2009; Kang et al.2010). However, as a kind of reinforced material with the steel bar or steel strand, the durability is threatened for that the prestressed bolt (cable) in the prestressed and severe surrounding rock environment for a long time.

Recently, the durability of the prestressed bolt (cable) has been highly concerned by scholars at home and abroad. The Fédération Internationale de la Précontrainte has collected and analyzed some major anchor bolt (cable) failure cases (Zeng et al. 2004; Zhang et al. 2001; Liu et al.2001); With the support of the US Department of Energy, Chandra et al.(2007) carried out the study of corrosion characteristics and mechanism of different anchor cables under the influence of nuclear waste in Yucca Mountain geological environment; Gamboa et al. (2003) studied the influence of environmental factors on the stress corrosion failure of the prestressed bolt through the indoor test for the first time. The research on the prestressed bolt started relatively late in China. Zheng et al. (2010) carried out the experimental research on the influence of environmental factors on mechanical properties of the bolt. Zhao et al.(2007) studied the factors affecting the durability of the bolt under the stress and environmental corrosion condition by indoor simulation test and field sampling test; Li et al. (2008) quantitatively described the influence of the pH value, time, stress level and other factors on the corrosion amount per unit length of the specimen through indoor accelerated corrosion test; Li et al. (2017) analyzed the influence characteristics of chloride ion concentration, time, pH value and other factors on

the corrosion of the cables and the mutual coupling relationship between different influencing factors through the indoor test; Zeng et al. (2011) studied the strength index and apparent characteristics of the anchor cable under strong corrosion environment; Zhang et al. (2018) observed the corrosion damage morphology of the prestressed anchor cable under different time, established the relationship between the indicators like corrosion pit area and depth and the time, and analyzed the surface damage evolution law of the stress corrosion.

At present, most of the research on rock bolt (cable) durability is limited to the indoor test of simulated corrosion environment, which is quite different from the actual working environment of the anchor bolt (cable). In this paper, the bolt samples obtained from a underground coal mine were used as the experimental object to study the corrosion characteristics through the macro observation and indoor weight loss method. Meanwhile, macro and micro means were adopted to analyze the failure mechanism of a certain cable sample in this mine.

2 Examination of rock bolt (cable) obtained from underground roadways

2.1 Sampling condition

The samples were taken from Qishan Coal Mine in Xuzhou, China. Qishan Coal Mine is a typical old mine, which was put into operation in December 1959. The influencing environmental factors such as temperature and humidity, pH value of seepage water, harmful ions, stray current, residual prestress and so on were tested before examination. It is found that the surrounding rock environment of the bolts (cables) is stable in the same horizontal stratum, which provides the possibility to study the corrosion behavior of the rock bolts with different service years. Six full-length adhesive samples were drilled in the -700m East Wing return airway. Fig. 1 shows the fielding sampling diagram. After the bolt (cable) samples were taken out, they were immediately packed and sealed with the plastic wrap in order to avoid the accelerated corrosion caused by the contact with air which would otherwise affect the test results. The samples obtained from underground coal mine were shown in Fig. 2 , which numbered as S-1, S-2, S-3, S-4, S-5, S-6 respectively. The details of bolt (cable) samples see Table 1.

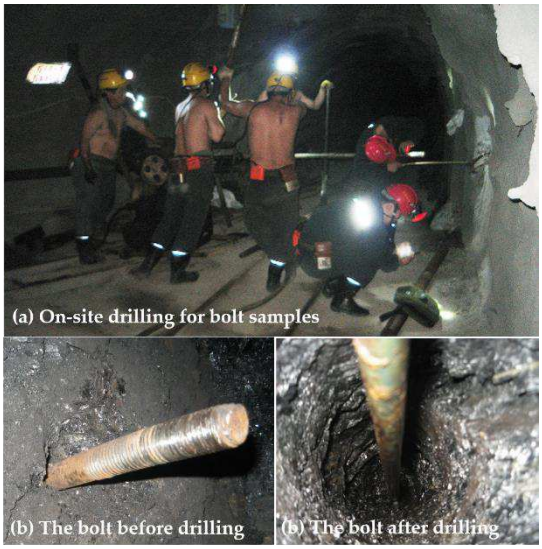

Figure 1 Field sampling diagram

Figure 2 Bolt (cable) samples

2.2 Corrosion behavior of bolt samples

The corrosion degree of five bolt samples which were not failed was analyzed, and the weight loss was measured on 2 cm samples taken respectively from the bolt head, free section and anchorage section. The bolt was derusted by acid pickling. Fig. 3 shows the schematic diagram of the bolt samples before and after derusting. The mass loss can directly and quantitatively characterize the corrosion degree of the bolt, which is calculated by Eq. (1), and the corrosion rate of the bolt is calculated by Eq. (2).

$$\Delta W = \frac{w_0 - w_1}{A_0} \pm \Delta W_{\mathrm{U}} \tag{1}$$

$$v_{\mathrm{corr}} = \Delta W / t \tag{2}$$

Where ΔW is the weight loss per unit area of the bolt; w_0 is the mass before derusting of the bolt; w_1 is the mass after derusting; A_0 is the surface area of the bolt; ΔW_{U} is the weight loss per unit area of the original stainless bolt after pickling, and

$\Delta W_U = W_{U0} - W_{U1}$; W_{U0} is the mass per unit area of the original stainless bolt before pickling; W_{U1} is the mass per unit area after pickling; v_{corr} is the corrosion rate of the bolt; and t is the service time of the bolt.

Table 1 The details of bolt (cable) samples

Sample	Bolt diameter / mm	Service period /Year	Residual prestress	Working environment					Sample morphological description
				Surrounding rock	Temperature	Humidity	seepage water PH	harmful ions	
S-1	20	1.5	≥70%	Coal	25.2	93.6	7.1	SO_4^{2-}、Cl^-	Greenish brown and Slightly uniform corroded, no failure
S-2	20	2.0	≥70%	Coal	24.9	90.8	7.4	SO_4^{2-}、Cl^-	Greenish brown and Slightly uniform corroded, no failure
S-3	20	3.0	≥70%	Coal	25.6	91.5	7.5	SO_4^{2-}、Cl^-	Greenish brown and Slightly pitting corroded, no failure
S-4	20	5.0	≥70%	Coal	24.8	93.2	7.2	SO_4^{2-}、Cl^-	Reddish brown and Severe pitting corroded, no failure
S-5	20	8.0	≥70%	Coal	25.2	92.9	7.4	SO_4^{2-}、Cl^-	Reddish brown and Severe pitting corroded, no failure
S-6	16	6.0	≥70%	Coal	24.9	93.3	7.6	SO_4^{2-}、Cl^-	Reddish brown and Severe pitting corroded, failure

As shown by the appearance of the bolt samples taken, all samples have slight corrosion, which can be divided into uniform corrosion and local pit corrosion. S-1 and S-2 are characterized by uniform corrosion, and pit corrosion occurs in different parts of S-3, S-4 and S-5. The number of corrosion spots on the surface of each samples increases with the increase of service time. For example, a large area of corrosion spots can be found on the surface of S-5 bolt which has been used for 8 years, and the depth of some pits reaches 0.18 mm.

(a) Bolt sample before derusting

(b) Bolt sample after derusting

Figure 3 Comparison of sample before and after derusting

Fig. 4 shows the time-mass loss relation diagram of different parts of the bolt. As shown in the figure 4, with the increase of service time, the corrosion amount of different parts of the bolt increases year by year. The corrosion amount of different parts is characterized by the rule of anchor head > anchor end > free section. This is because the anchor head has been exposed to the air for a long time, and the O_2 in the air accelerates the corrosion of the anchor head, while other parts are wrapped by concrete mortar for a long time with less contact with corrosive media, so the corrosion is relatively light in degree.

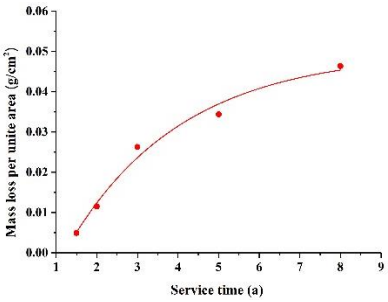

(a) Free section

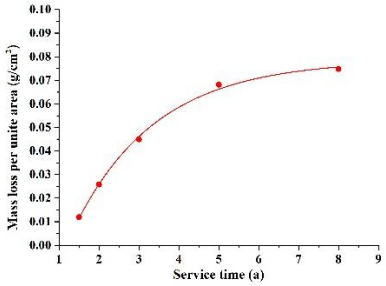

(b) anchor end

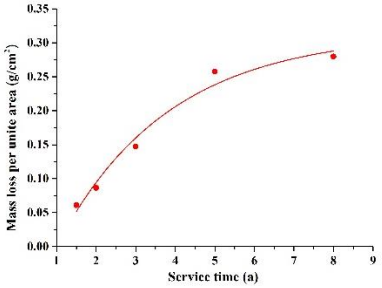

(c) anchor head

Figure 4 Time-mass loss relationship of different parts of the bolt

Fig. 5 shows the variation curve of the corrosion rate of different parts of the bolt. As shown in Fig. 5, the corrosion rate of each part of the bolt increases rapidly in the early stage and slows down in the later stage. The reason is that with the increase of service time, the corrosion on the surface of the bolt is accumulated, which avoids the large area contact between the bolt body and external corrosion factors, thus reducing the growth rate of bolt corrosion.

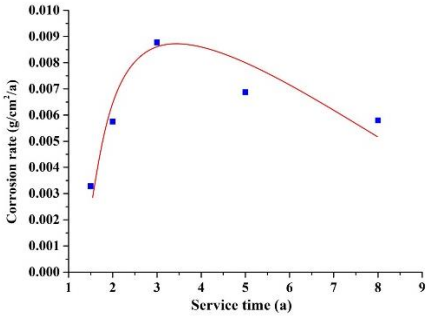

(a) Free section

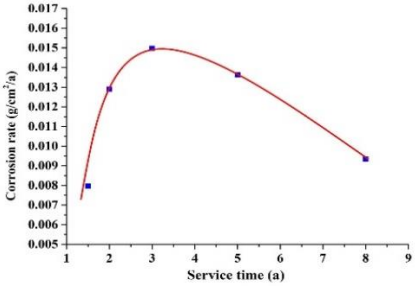

(b) anchor end

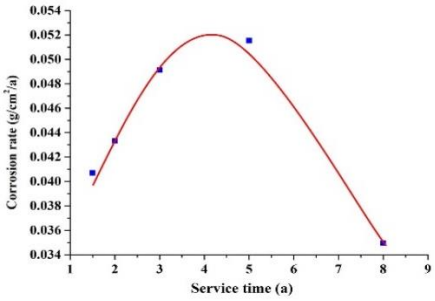

(c) anchor head

Figure 5 Variation of coronation rate in different parts of the bolt

2.3 Examination of the microstructure of the fracture surface

2.3.1 Macroscopic analysis of the sample fracture

The failure analysis of the anchor cable sample S-6 in use for six years in Qishan Coal Mine was conducted. Fig. 6 shows the overall morphology of S-6. The anchor cable has brown surface and consists of seven steel strands. The corrosion morphology of each area of the broken anchor cable sample is shown in Fig. 7. The macro analysis results show that the whole anchor cable is characterized by uniform oxidation corrosion (Fig. 7a). Pit corrosion is found in some areas of the steel strand in the region from about 900mm away from the anchorage to the fracture, as shown by the arrow in Fig. 7 (b). However, near the fracture (about 1200mm away from the anchorage), the number and degree of pit corrosion are relatively serious, and some places even have spalling (Fig. 7c). As shown in Fig. 7(c), the length of the steel strand at the breaking point of the anchor cable is different. It is an inclined fracture formed under tensile stress with a certain angle to the axial direction, and the longitudinal length of the fracture is about 25 mm. There is no obvious necking before fracture of these steel wires, and it can be observed that the steel strands crack from the outer surface with more serious oxidation and corrosion.

Figure 6 morphology of the broken anchor cable: (a) Longitudinal morphology (b) Transverse section morphology

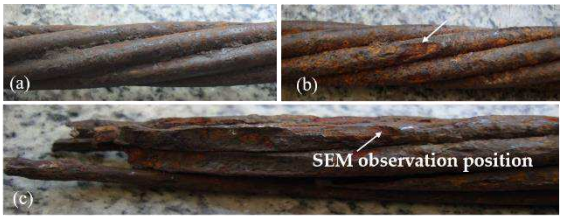

Figure 7 Macro fracture corrosion morphology of the anchor cable: (a) the steel strand near anchorage (b) the steel strand near anchorage about 900mm away from anchorage (c) Fracture position

2.3.2 Microscopic analysis of corrosion products of sample fracture

(1) Analysis of corrosion products on and near fracture surface

The macroscopic and microscopic fracture morphology analysis was carried out after the position marked with white words was cleaned in Fig. 7. The microscopic corrosion product morphology and EDS energy spectrum composition analysis on the fracture surface are as shown in Fig. 8. The microscopic analysis results of the fracture show that the fracture surface is mainly covered by iron oxide, and sulfur corrosion products are detected in local area.

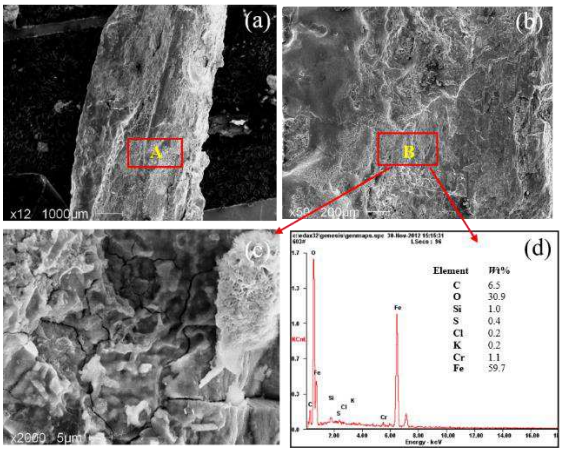

Figure 8 Morphology and EDS analysis of fracture surface corrosion products: (a) With 12 times magnification; (b) Point A with 50 times magnification; (c) Point B with 2000 times magnification; (d) EDS analysis

The morphology of microscopic corrosion products on the fracture edge surface and EDS energy spectrum composition analysis are shown in Fig. 9. The results show that the corrosion products are mainly in fluffy needle and ball shape. The main components of the corrosion products as detected are Fe, O, Cl, S, Si, Mn, Cr, etc. The content of element Cl in the corrosion products is as high as 4.4%, and the mass content of element S is 0.6%.

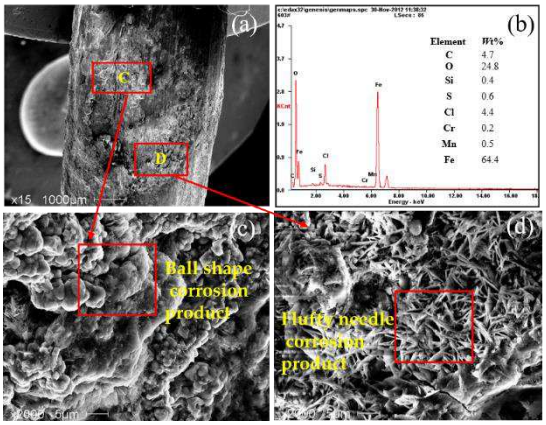

Figure 9 Morphology and EDS analysis of surface corrosion products near the fracture: (a) With 15 times magnification; (b) EDS analysis; (c) Point C with 2000 times magnification; (d) Point D with 2000 times magnification;

(2) Analysis of corrosion products on fracture and steel strand profile

The metallographic samples of transverse section were taken from the pit corrosion area about 900 mm away from the anchorage near the non-fracture area. After sample grinding and polishing, the morphology was observed by the scanning electron microscope and the EDS energy spectrum composition was analyzed. Fig. 10 shows the low speed fracture of the steel wire, and Fig. 11 (a), (b) and (c) show the microscopic morphology and composition analysis of corrosion products of the area near the matrix, near the surface and inside the matrix of the reinforcement in the area with pit corrosion. Fig. 12 shows the microscopic morphology and composition analysis of corrosion products of the area near the matrix, near the surface and inside the matrix of the reinforcement in the area without pit corrosion. The analysis results show that the depth of some pits reaches 0.9 mm. In the pit corrosion area, the corrosion products containing O, Cl and S or O and S are found near the

steel strand matrix and the surface; in the area without pit corrosion, the corrosion products containing O are mainly found near the steel strand matrix and the surface.

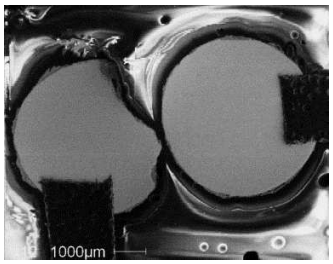

Figure 10 Low-power images of metallographic samples of transverse section of steel strand with and without pit corrosion

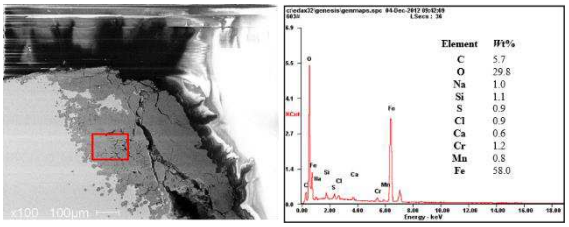

(a) Composition of corrosion products near the matrix in pit corrosion area

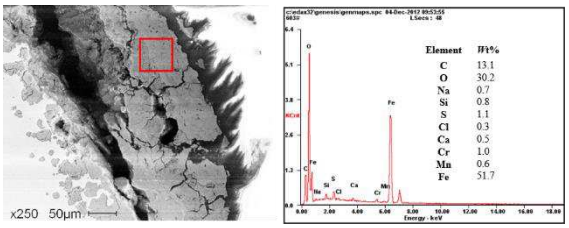

(b) Composition of near surface corrosion products in pit corrosion area

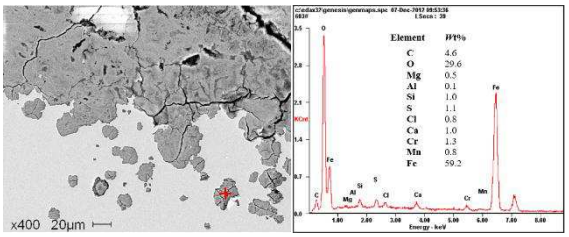

（c）Composition of point corrosion products in matrix

Figure 11 EDS energy spectrum analysis of corrosion products in pits of metallographic samples of transverse section

2.3.3 Sample failure mechanism

As known from the macroscopic and microscopic analysis of the samples, the failure samples are not characterized by obvious plastic deformation or necking, which indicates that the failure mode of the sample is brittle failure. The fracture path profile of the sample can be devided into three stages, as shown in Fig 13. In first stage, there is a shallow crack perpendicular to the applied load in the fracture initiation area (Fig 13a). Then the crack deflects and propagates along the longitudinal direction in second stage (Fig 13b). Lastly, the sample was suddenly fractured with higher deviation angle in third stage (Fig 13c). This type of failure has also been observed in other research results (Proverbio et al. 2003; Toribio et al 2010; Perrin et al 2010), which is considered to be a typical feature of SCC. Therefore, to sum up, the failure samples have been in the O, Cl and S surrounding rock environment for a long time, which results in pit corrosion, causes the corrosion and spalling of surface material of the steel strand, reduces the outer diameter of the anchor cable and its bearing capacity, and leads to one-time SCC fracture of the anchor cable.

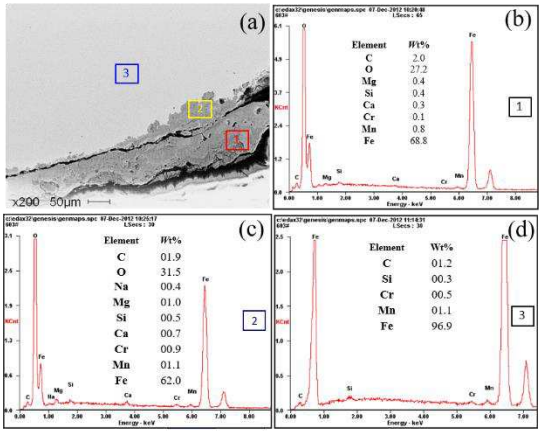

Figure 12 EDS energy spectrum analysis of corrosion products in the area without pits of transverse section：（a）Corrosion morphology（b）Composition of near surface corrosion products；（c）Composition of corrosion products near the matrix ；（d）Composition of corrosion products in matrix

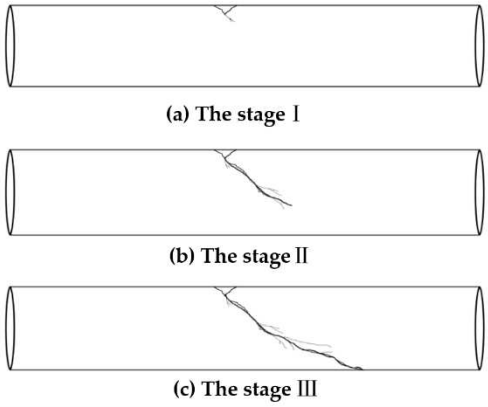

Figure 13 The fracture path profile of S-6

3. Conclusions

The corrosion behavior and failure mechanism of bolt (cable) samples obtained from a certain mine were analyzed. The conclusions are as follows:

(1) The corrosion forms of the samples are divided into uniform corrosion and local pit corrosion. The main corrosion form of S-1 and S-2 is uniform corrosion, which have short service time; But for S-3, S-4 and S-5, which with longer service time, experience different degrees of pit corrosion, and the number of corrosion spots on the bolt surface increases with the increase of service time.

(2) The corrosion amount of different parts of the bolt features the rule of anchor head > anchor end > free section. The corrosion amount of the bolt increases with the increase of service time, but the corrosion rate increases rapidly in the early stage and slows down in the later stage.

(3) The failure mechanism of sample S-6 is that it has been in the surrounding rock environment of O, Cl and S for a long time, resulting serious pitting corrosion and spalling of the surface material of the steel strand, which reduces the outer diameter of the rock cable and its bearing capacity, finally leads to the instantaneous SCC fracture of the sample S-6.

Acknowledgments: This research was supported by the Science and Technology Project of Langfang City (2020013039), the Special Fund of Basic Research and Operating of North China Institute of Science & Technology (Grant Nos. 3142020001), and the State Scholarship Fund of China.

References

Hu D et al (1987) Application of anchorage technology on geotechnical engineering. China Building Industry Press.

Zhang J, Han L, Zhu BZ, Zeng HH (2009) The problems related to the anchorage engineering for side slop and their effects. Journal of Railway Engineering Society 1:7-31.

Kang HP, Wang JH, Lin J (2010) Study and applications of roadway support techniques for coal mines. Journal of China Coal Society 35:1809-1814.

Zeng XM，Chen ZY，Wang JT，Du YH (2004). Research on safety and durability of bolt and cable-supported structures. Chinese Journal of Rock Mechanics and Engineering 23:2235−2242.

Zhang M (2001). Safety and durability analysis of china railway tunnel structure. Engineering Technology BBS: Civil Structural Engineering the Security and the Durability. Beijing: Tsinghua University press.

Liu XL (2001) Fundamental research of structural engineering durability. Engineering Technology BBS: Civil Structural Engineering the Security and the Durability. Beijing: Tsinghua University press.

Dhanesh C, Jack D (2007) Sub-surface corrosion research on rock bolt system，Perforated SS Sheets and Steel Sets for the Yucca Mountain Repository Quarterly Technical Report. Las vegasa: University of Nevada 12:10-15 .

Erwin G, Andrej A (2003). Environmental influence on the stress corrosion cracking of rock bolts. Engineering Failure Analysis 10:521–558.

Zheng J, Zeng HH，Zhu BZ (2010) Test study of influence of erosion on mechanical behavior of anchor. Chinese Journal of Rock Mechanics and Engineering 29:2469-2474.

Zhao J, Ji WZ, Zeng XM, Liang B, Zhong B, Xu JX (2007) Experimental study on durableness of anchor with stress corrosion. Chinese Journal of Rock Mechanics and Engineering S1:3427-3431.

Li YY (2008) Study on long term stability of geotechnical prestressd anchor system. Beijing: Beijing Jiaotong University.

Li HS (2017) The corrosion regularity and durability of prestressed anchor. Handan: Hebei University of Engineering.

Zeng HH，Zhu BZ，Gao ZH (2011) Experimental study on strength characteristics of cable under powerful corrosion. Journal of Water Resources and Architectural Engineering 9: 48-52.

Zhang SF, Chen XQ, Han B ,Qi H (2018) Study on corrosion damage evolution mechanism of geotechnical prestressed anchor cable. Journal of Shandong Jianzhu University 33:1-6+14.

E. Proverbio, P. Longo (2003) Failure mechanisms of high strength steels in bicarbonate solutions under anodic

polarization, Corros. Sci. 45:2017–2030.

J. Toribio, B. González, J. Matos (2010) Fatigue and fracture paths in cold drawn pearlitic steel, Eng. Fract. Mech. 77:2024–2032.

M. Perrin, L. Gaillet, C. Tessier, H. Idrissi (2010) Hydrogen embrittlement of prestressing cables, Corros. Sci. 52:1915–1926.

Figures

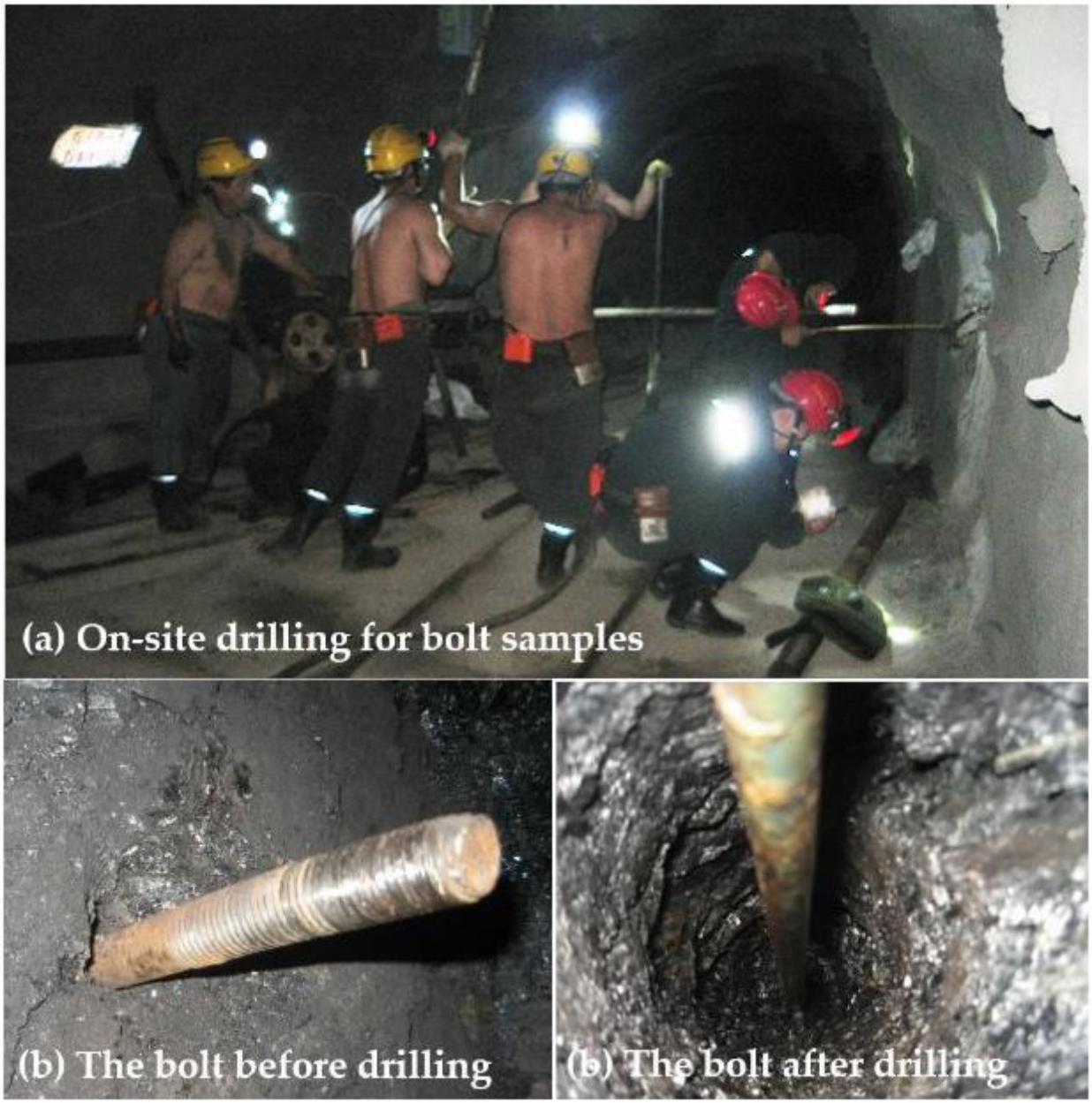

Figure 1

Field sampling diagram

Figure 2

Bolt (cable) samples

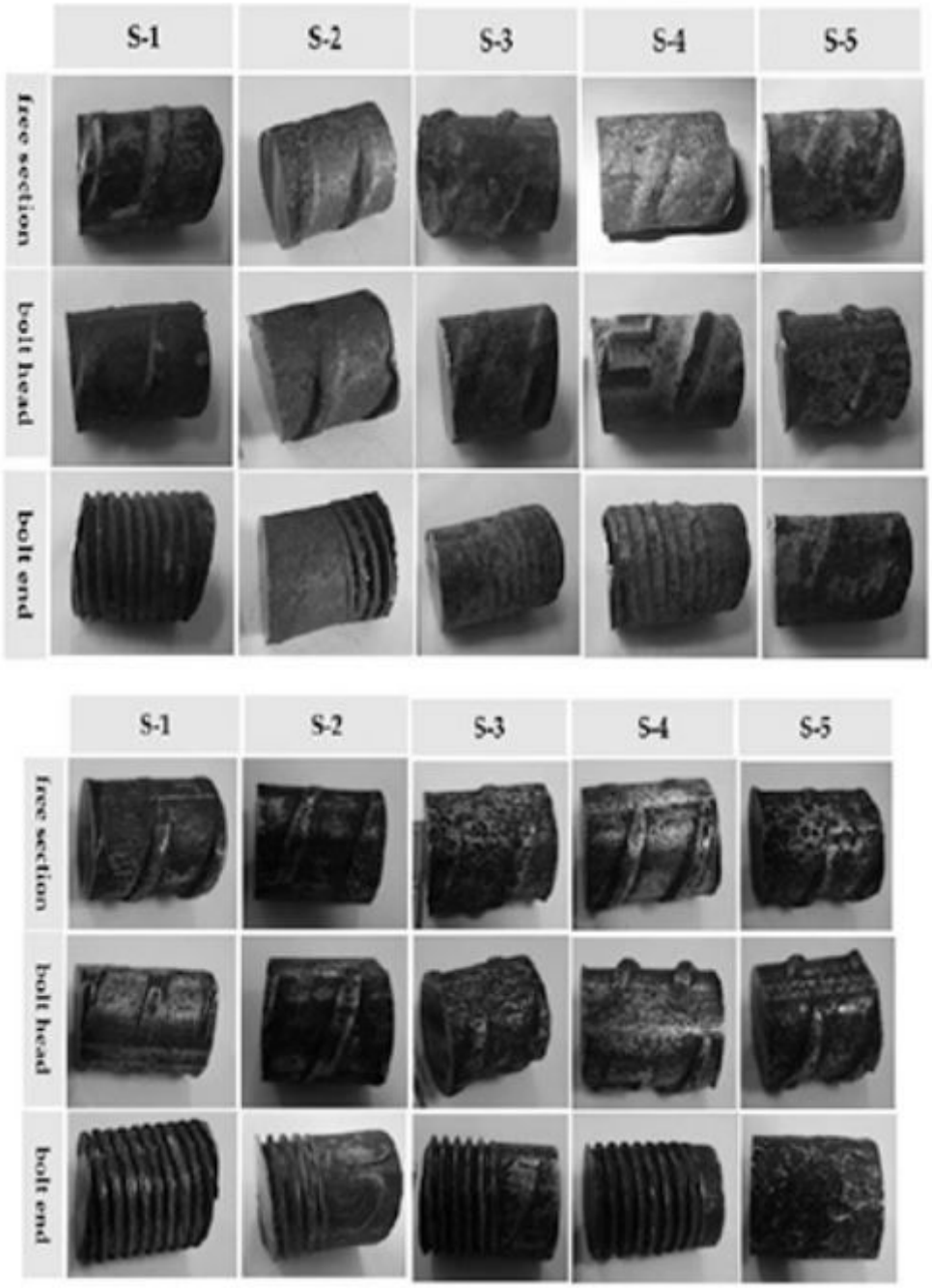

Figure 3

Comparison of sample before and after derusting

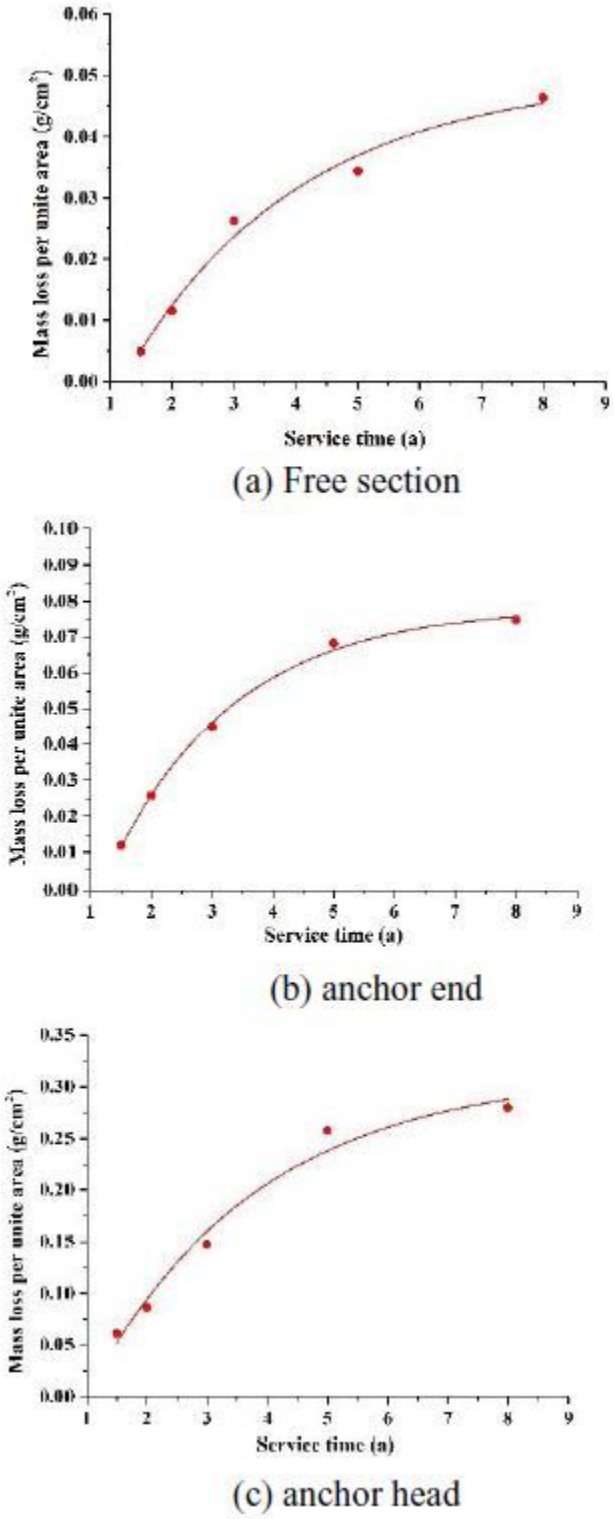

Figure 4

Time-mass loss relationship of different parts of the bolt

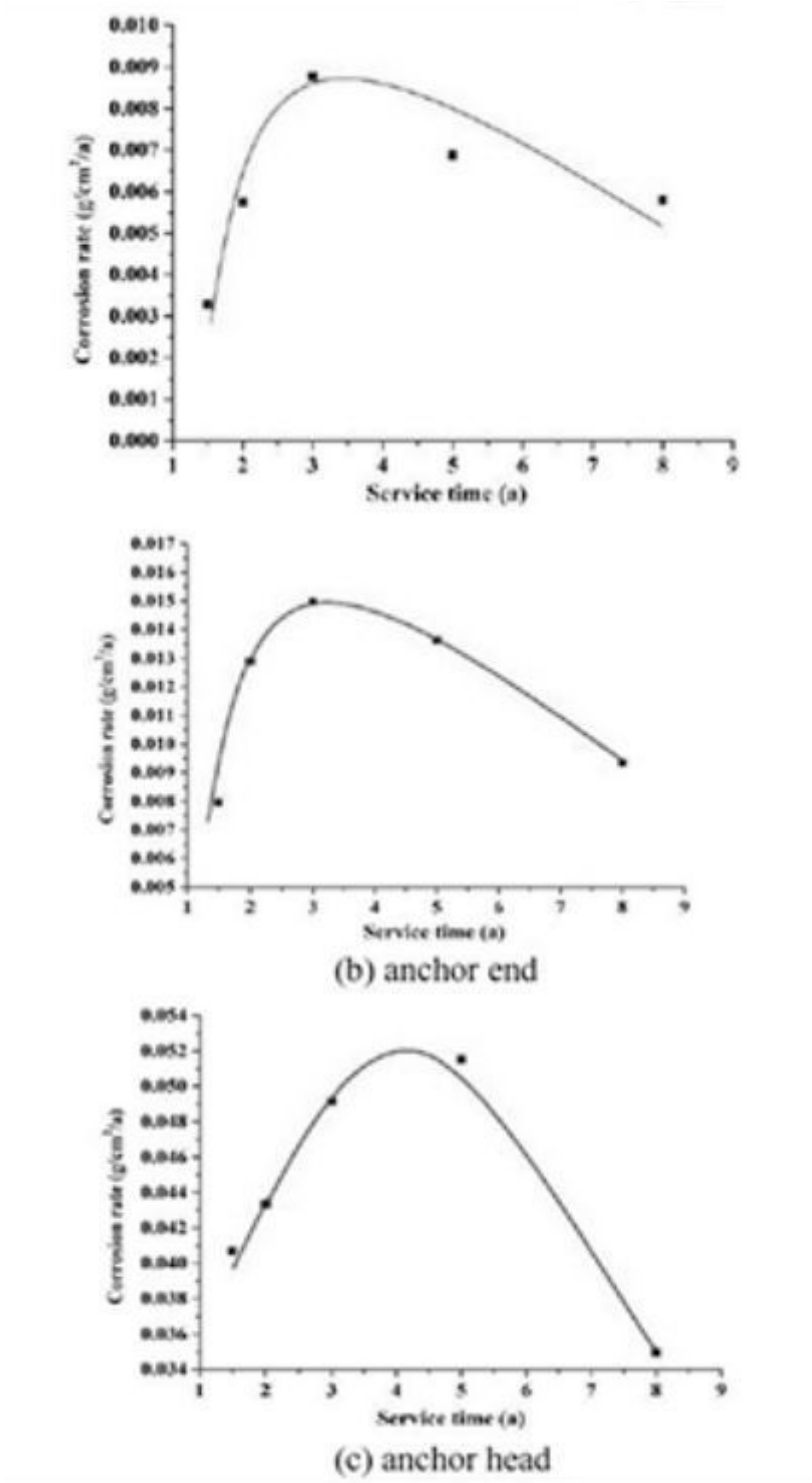

Figure 5

Variation of coronation rate in different parts of the bolt

Figure 6

morphology of the broken anchor cable: (a) Longitudinal morphology (b) Transverse section morphology

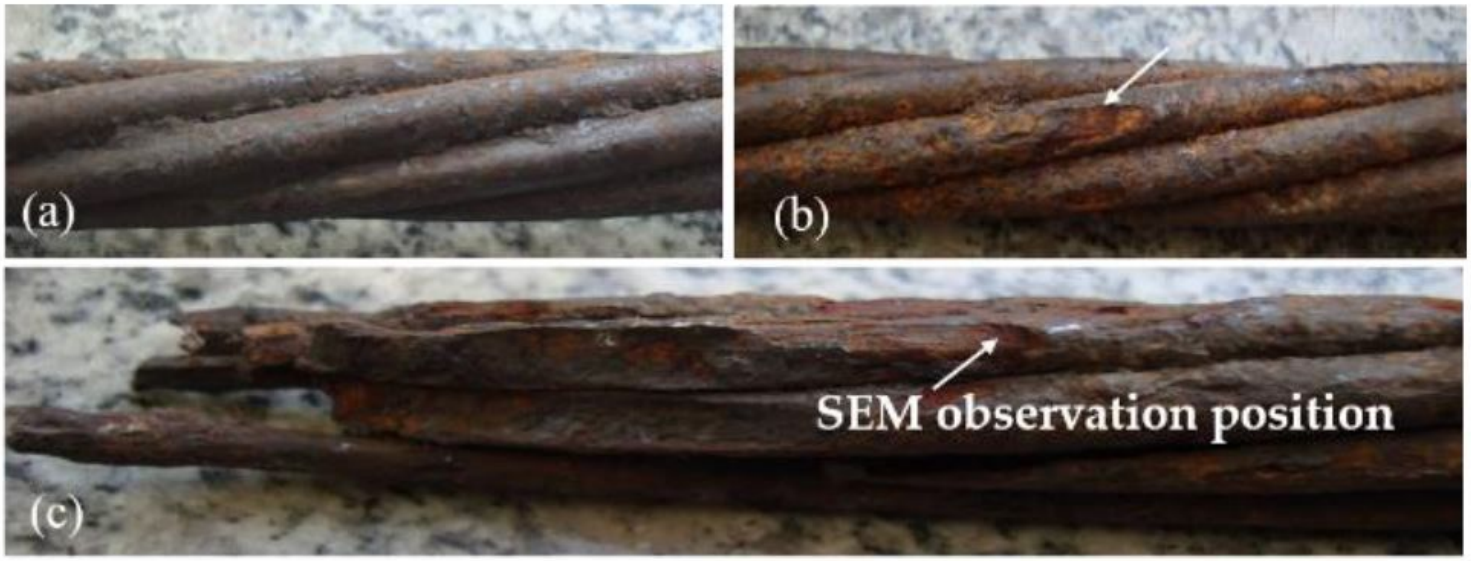

Figure 7

Macro fracture corrosion morphology of the anchor cable: (a) the steel strand near anchorage (b) the steel strand near anchorage about 900mm away from anchorage (c) Fracture position

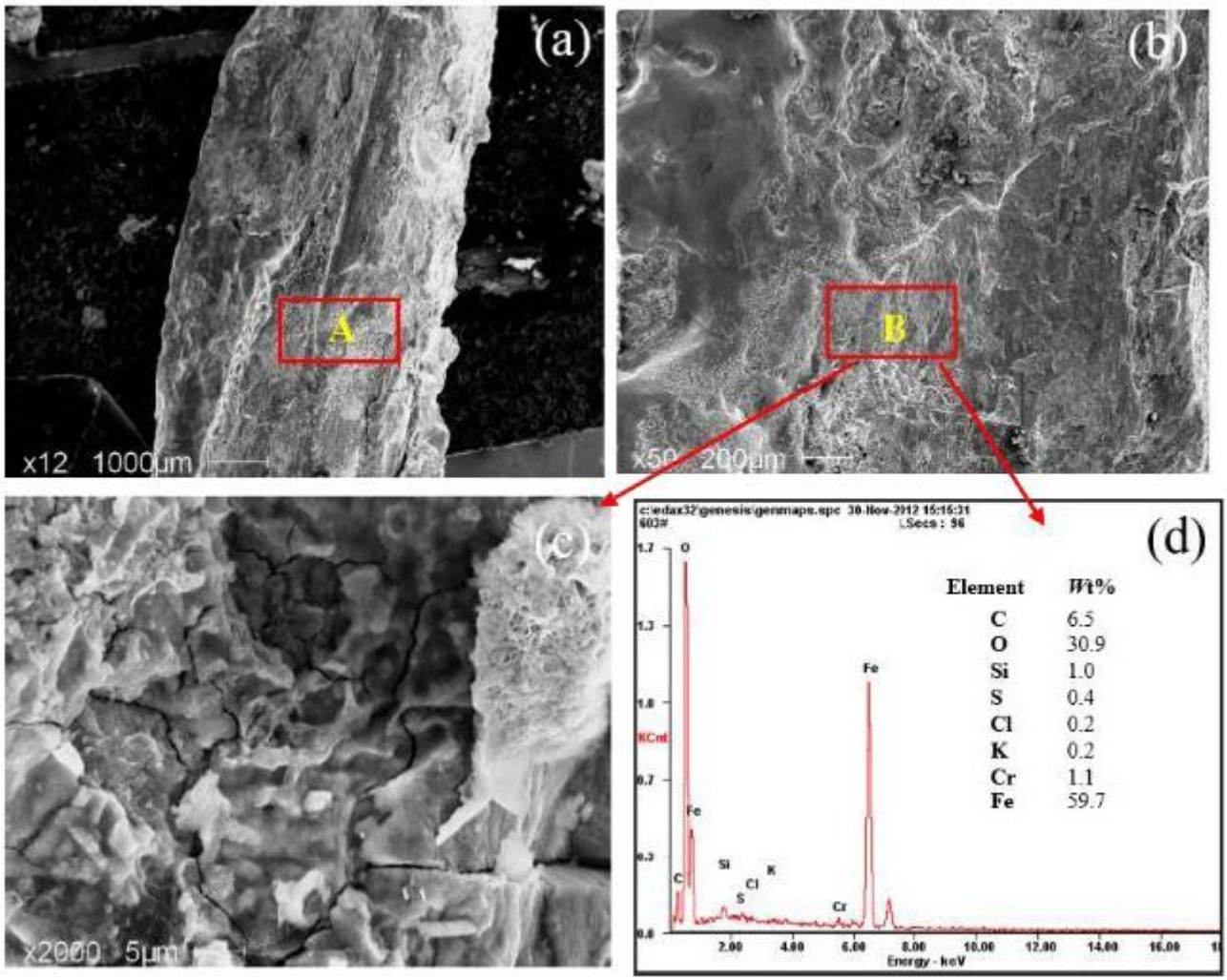

Figure 8

Morphology and EDS analysis of fracture surface corrosion products: (a) With 12 times magnification; (b) Point A with 50 times magnification; (c) Point B with 2000 times magnification; (d) EDS analysis

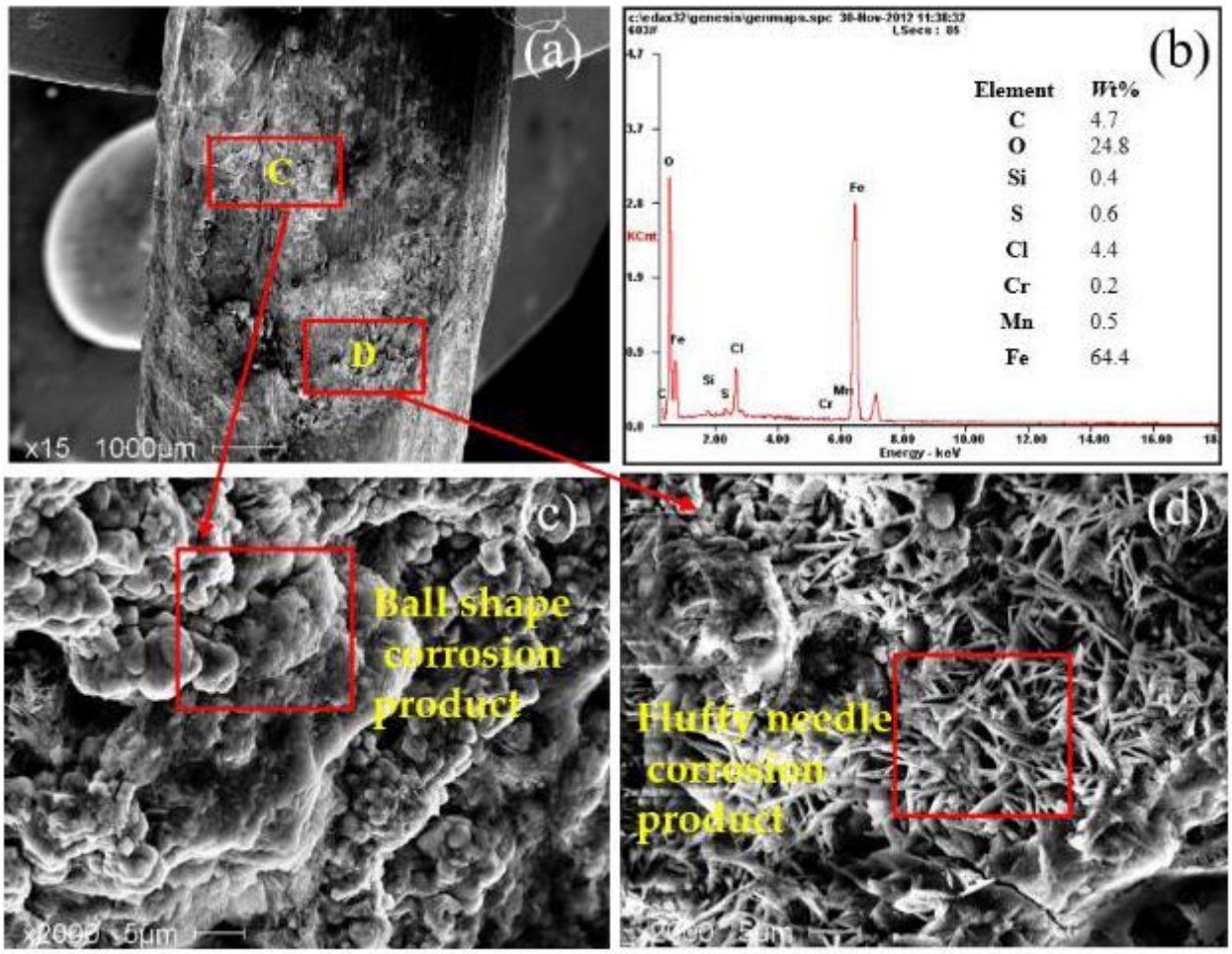

Figure 9

Morphology and EDS analysis of surface corrosion products near the fracture: (a) With 15 times magnification; (b) EDS analysis; (c) Point C with 2000 times magnification; (d) Point D with 2000 times magnification;

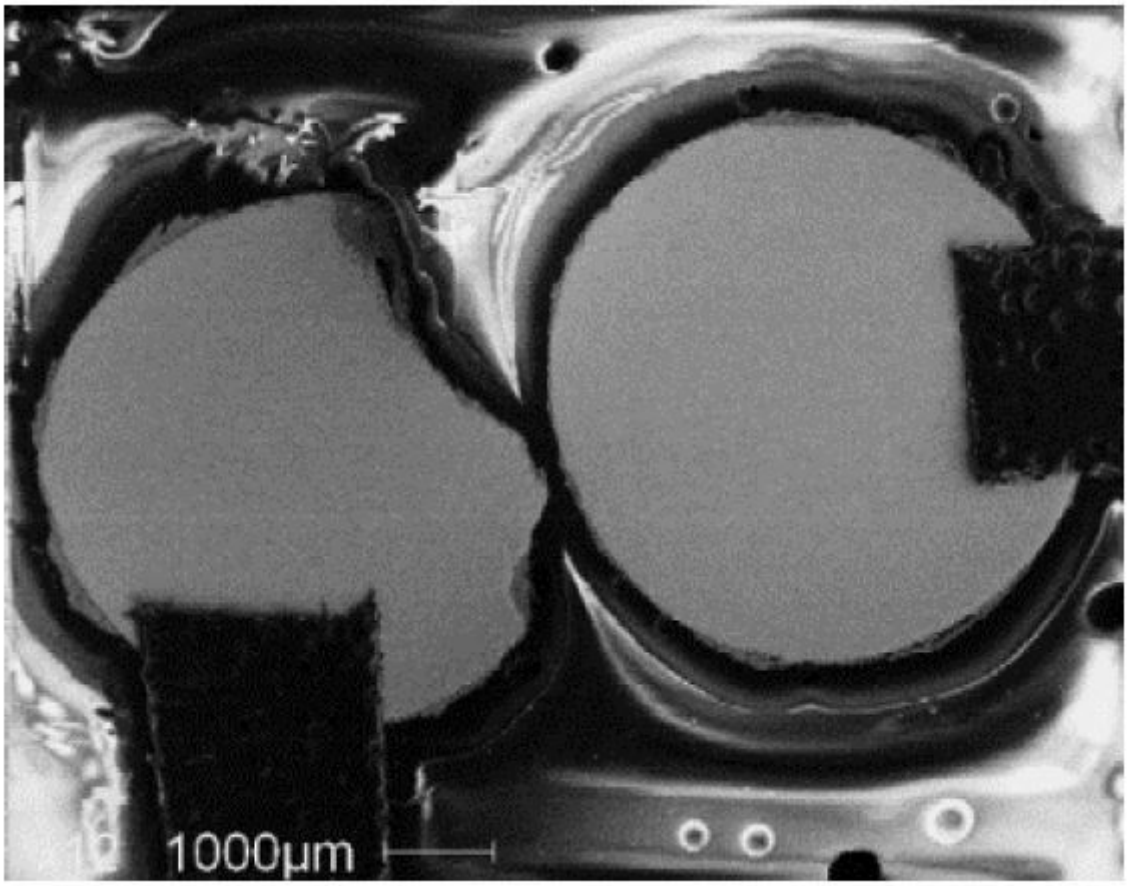

Figure 10

Low-power images of metallographic samples of transverse section of steel strand with and without pit corrosion

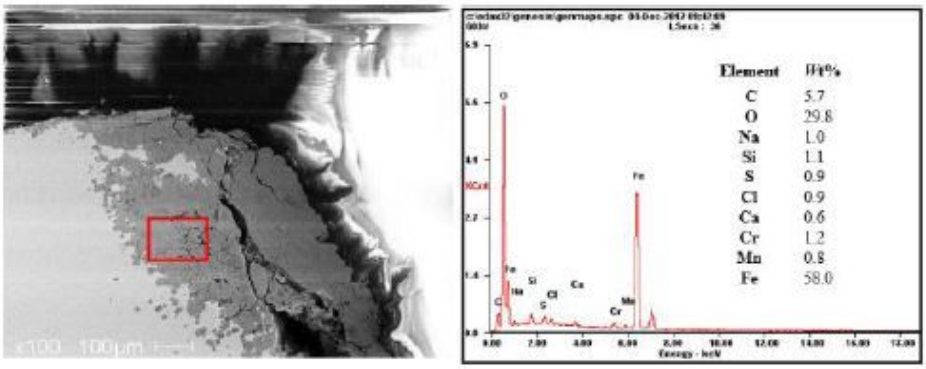

(a) Composition of corrosion products near the matrix in pit corrosion area

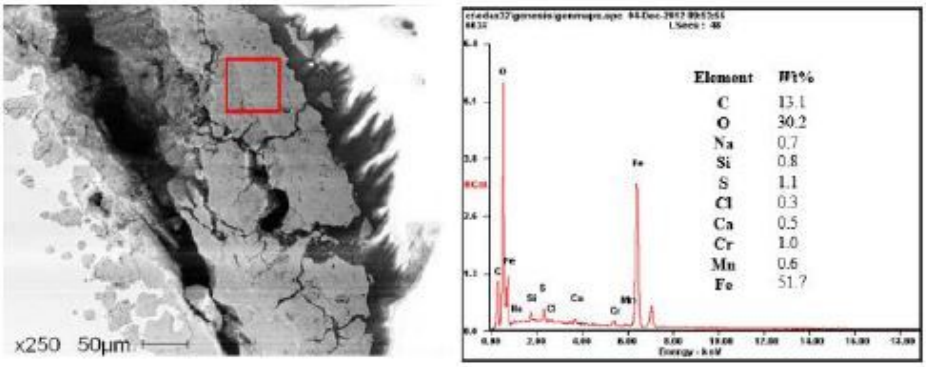

(b) Composition of near surface corrosion products in pit corrosion area

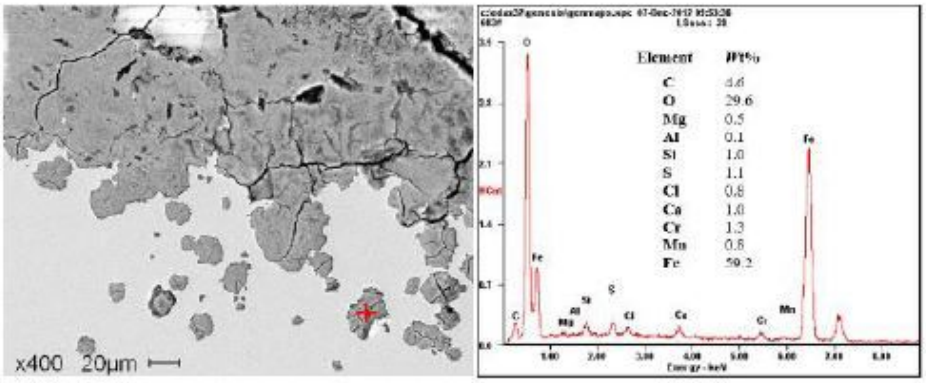

（c）Composition of point corrosion products in matrix

Figure 11

EDS energy spectrum analysis of corrosion products in pits of metallographic samples of transverse section

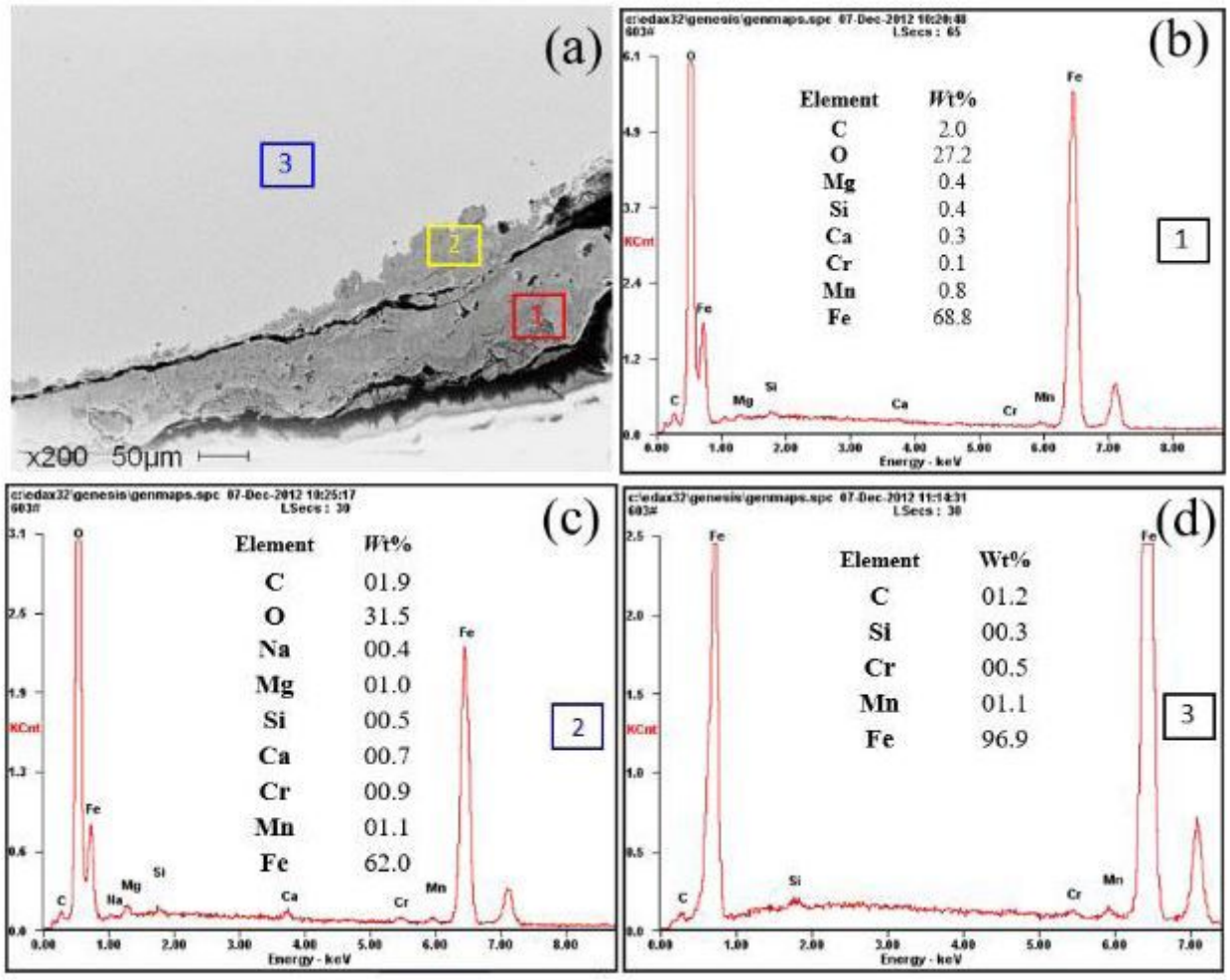

Figure 12

EDS energy spectrum analysis of corrosion products in the area without pits of transverse section（a） Corrosion morphology（b）Composition of near surface corrosion products（c）Composition of corrosion products near the matrix （d）Composition of corrosion products in matrix

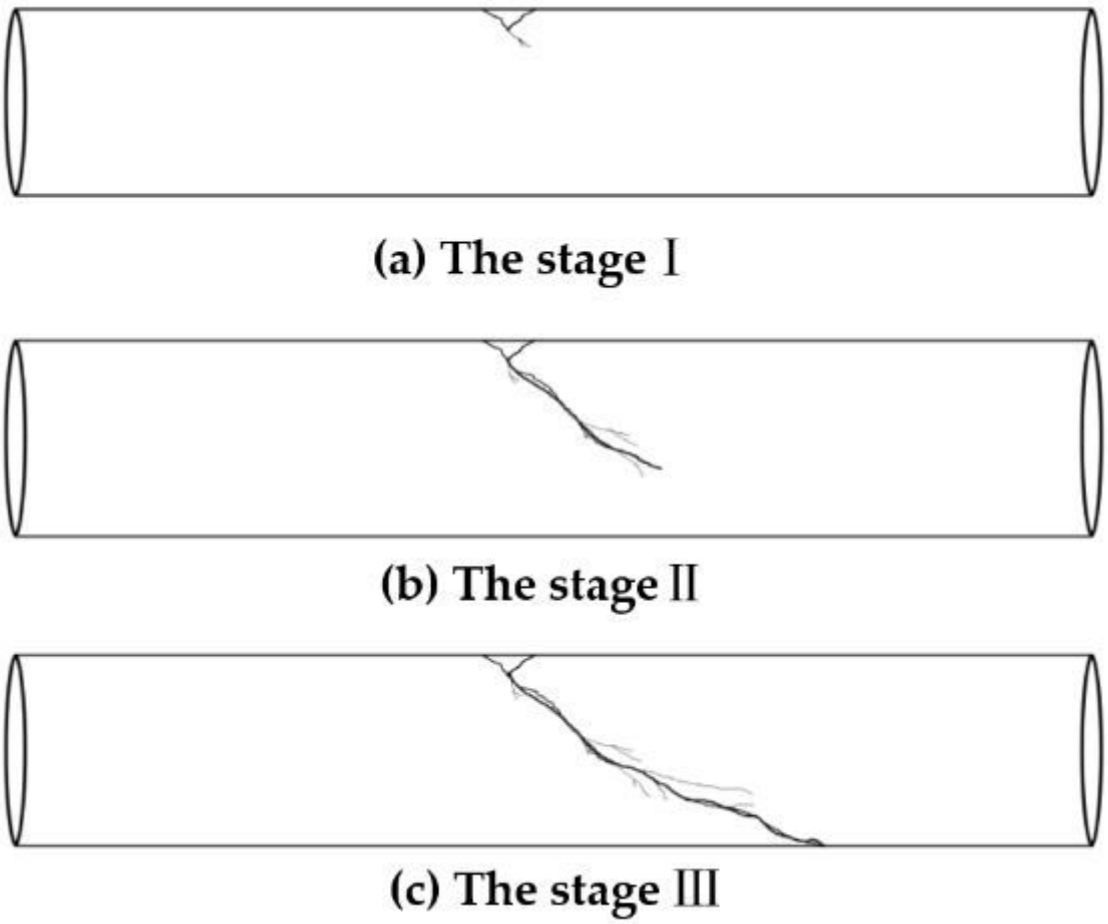

Figure 13

The fracture path profile of S-6